Heliyon 8 (2022) e09772

Contents lists available at ScienceDirect

Heliyon

journal homepage: www.cell.com/heliyon

Research article

Anisotropy in the peripheral visual field based on pupil response to the glare illusion

Novera Istiqomah [a,b], Yuta Suzuki [a,c,*], Yuya Kinzuka [a], Tetsuto Minami [a], Shigeki Nakauchi [a]

[a] Department of Computer Science and Engineering, Toyohashi University of Technology, Toyohashi, Aichi, Japan
[b] Department of Computer Engineering, Telkom University, Bandung, West Java, Indonesia
[c] NTT Communication Science Laboratories, NTT Corporation, Atsugi, Kanagawa, Japan

ARTICLE INFO

Keywords:
Brightness perception
Glare illusion
Pupillometry
Peripheral visual field
Anisotropy

ABSTRACT

Visual-field (VF) anisotropy has been investigated in terms of spatial resolution of attention, spatial frequency, and semantic processing. Brightness perception has also been reported to vary between VFs. However, the influence of VF anisotropy on brightness perception using pupillometry has not been investigated. The present study measured participants' pupil size during glare illusion, in which converging luminance gradients evoke brightness enhancement and a glowing impression on the central white area of the stimulus, and halo stimuli, in which the same physical brightness of the glare illusion is used with a diverging luminance pattern. The results revealed greater stimulus-evoked pupillary dilation and glare-related dilated pupil reduction in the upper VF (UVF) compared with other VFs and halo-related pupillary changes, respectively. The stimulus-evoked pupillary dilation was affected by poor contrast sensitivity. However, owing to the superior cognitive bias formed by statistical regularity in natural scene processing of the glare illusion in the UVF, we found reduced pupillary dilation compared with the response to halo stimuli and the response from other VFs. These findings offer valuable insight into a method to reduce the potential glare effect of any VF anisotropy induced by the glare effect experienced in daily vision. An important practical implication of our study may be in informing the design of applications aimed at improving nighttime driving behavior. We also believe that our study makes a significant contribution to the literature because it offers valuable insights on VF anisotropy using evidence from pupillometry and the glare illusion.

1. Introduction

The difference of observers' perception scale (slightly or significantly) in different visual fields (VFs) associated with the stimulus orientation is termed as VF anisotropy. Multiple studies have demonstrated VF anisotropy in visual perception [1, 2, 3, 4]. For example, the spatial resolution of attention and spatial frequency sensitivity are known to have an advantage in human vision, attributed to a downward bias in the lower VF (LVF) compared with the upper VF (UVF) [5]. In contrast, an advantage in the UVF is also reported in motor-related tasks, visual search tasks, and semantic understanding [6, 7, 8]. In the context of bioecology, an object presented in the lower and upper hemifield is perceived as being placed closer and farther in space, respectively. This vertical VF segmentation may be enhanced by the function that enables individuals to experience a critical event more easily close-up for them to survive in the natural environment, whereas objects farther away need to be predicted accurately from a distance [9, 10]. These specific functions of vertical VFs have also been discussed from physiological perspectives. Specifically, previous studies that adapted pupillometry have suggested a higher pupil sensitivity to light changes in the UVF during an attention task [11, 12, 13, 14, 15, 16, 17].

Apparent brightness perception is reported to vary between VFs [18]. Brightness perception in the visual system is determined by a confluence of the physical intensity of light and several context-dependent factors. Thus, brightness perception does not always match the quantity of physical light from the source. McCourt et al. (2013) conducted an illumination intensity matching task and reported that an illuminated object from the LVF is perceived as more illuminated compared with an illuminated object from the UVF owing to light adaptation that takes more time [19]. This mismatch between subjective brightness and physical luminance intensity has also been seen in the phenomenon of a larger pupillary constriction evoked by a bright

* Corresponding author.
E-mail address: yuuta.suzuki.fc@hco.ntt.co.jp (Y. Suzuki).

https://doi.org/10.1016/j.heliyon.2022.e09772
Received 15 January 2022; Received in revised form 9 March 2022; Accepted 17 June 2022

illusion [20], the sun's image [19], or a painting depicting the sun [21] that appears perceptually brighter.

Pupillometry, the measurement of pupil size, is a physiological index that reflects multiple cognitive states across species. Parts of the autonomic nervous system and the parasympathetic and sympathetic nervous systems regulate the iris sphincter and dilator muscles, respectively [22, 23, 24, 25, 26, 27]. Apart from functioning as a reflex to light, the pupil also reacts to subjective brightness perception. Laeng and Endestad (2012) initially reported that an optical illusion in which an object appears brighter than its physical luminance evokes larger pupil constriction [20]. This optical illusion is called the "glare illusion" and provokes robust brightness enhancement by a luminance gradient that converges toward the center of the pattern [28, 29]. Zavagno et al. found that the illusory perception emerged from the luminance gradient that caused not fully segregate the background and target area conducting the rating task experiment between the areas using luminance contours, illusory contours, no contours, and ambiguous contours [30]. The results were highly influenced by the process of segregation between the target area and the background combined with the luminance gradient attendance. Furthermore, previous research also used a glare illusion with "blue" converging gradients, which was subjectively evaluated as the brightest condition in a psychophysical adjustment task and elicited the most significant changes in large pupil constriction compared with other colors [28]. Part of the brightness enhancement may be attributed to the cognitive bias formed by statistical regularity in natural scene processing: the cognitive bias created by the visual property difference that ensues in natural scenes where "the sun shining in the blue sky" may be associated with the blue glare illusion and induce prominent pupil constriction [28].

The extent to which brightness perception is induced by VF anisotropy remains unclear. Specifically, it is unclear how the predominant understanding of ecologically explained cognitive bias, formed by statistical regularity in natural scenes in the VF (e.g., the light-from-above bias), affects brightness perception. Therefore, this study aimed to elucidate if visual processing conveying a dazzling effect in the glare illusion also has an ecological advantage in the VF.

We compared pupil size changes as stimuli (glare illusion and halo stimuli) were presented for a few seconds in five VF locations (upper, lower, left, right, and center). The changes in pupil size were regarded as an index of subjective brightness perception. From both ecological and anatomical points of view, pupillary response to the glare illusion was expected to vary across different VFs. We hypothesized that the differences in pupil changes between the glare illusion and halo stimuli in the UVF would be larger than those in the other positions owing to ecological factors, such as the representation of the sun and assumptions that the light source is in the UVF [29, 31]. Additionally, constricted pupils may occur in response to stimuli in the LVF owing to the advantage of spatial resolution and visual accuracy in the LVF [11, 32]. Thus, this research integrated pupillometry as an index of subjectively perceived brightness in anisotropic fields, especially focusing on the effect of the vertical hemifield.

2. Methods

2.1. Participants

Twenty-two undergraduate and graduate students (9 men and 13 women), aged between 23 and 33 years (mean = 26.86, SD = 3.90 years), participated in the experiment. All participants had normal or corrected-to-normal vision. Two participants were excluded from the analysis for recording 50% more eye blinks in all trials or invalid trials, the data of which could not be interpolated at the pre-processing stage. All experimental procedures were conducted according to the ethical principles outlined in the Declaration of Helsinki and approved by the Committee for Human Research at the Toyohashi University of Technology. The experiment was conducted with complete adherence to the approved guidelines of the committee. Informed written consent was obtained from the participants after procedural details had been explained to them. The raw data and analysis codes are available at https://github.com/suzuki970/GlarePupilAnisotropy.

2.2. Stimuli and apparatus

We used the achromatic glare illusion, which had eight circles of luminance gradation converging from the periphery to the center white region of the stimulus (which is a similar design to "*phantom illumination*" figure [33]). We also used a pattern with a diverging luminance pattern by rotating 180° the same gradient luminance of glare illusion as a control referred to as the halo stimuli (Figure 1A) [28,34]. This particular type of glare/halo stimuli has many advantages compared to the Asahi glare illusion and the ring-shaped glare illusion. The areas of the foveal and peripheral regions in the inverted Asahi glare illusion are not identical. Therefore, adjusting the global luminance of the Asahi glare illusion and its inverted form to the same values would be difficult. In comparison, the ring-shaped glare illusion and its inverted form would result in the same issue as the Asahi glare illusion.

The achromatic points of the stimuli's luminance gradation were 0.2959 and 0.3249 in the CIE1931 color space, while the luminance of Y changed linearly from 0.4218 cd/m^2 to 93.45 cd/m^2. The luminance of the background and center white region of the stimuli were 53.30 cd/m^2 and 93.45 cd/m^2, respectively. The spectral power distribution of the glare illusion's area and background (Figure 1B) was measured by a spectroradiometer (SR–3AR, TOPCON, Tokyo, Japan). The stimulus size and configuration were identical to those used by Suzuki et al. (2019). The center condition (i.e., the stimulus was presented in the center of the VF) contained eight circles with luminance gradation, with each circle located 4.62° from the center of the screen (Figure 1C). The diameter of each gradation circle was the visual angle of 3.62°. In the periphery condition (i.e., the stimulus was presented in the upper, lower, left, or right VF), the glare illusion and halo stimuli were located 8.35° from the screen's center, keeping the exact configuration of the stimulus luminance and size as in the center condition. We included a fixation point of 0.1° positioned at the center of the screen in both the center and periphery conditions. Thus, participants looked at the stimuli with their peripheral vision in the periphery condition. The experiment was conducted using MATLAB R2019b (MathWorks, Natick, MA) and Psychtoolbox [35]. All stimuli were presented on a liquid-crystal display (LCD) monitor (Display++, Cambridge Research Systems Ltd., Kent, UK) with a resolution of 1920 × 1080 pixels and a refresh rate of 120 Hz.

2.3. Procedure

Participants rested their chin at a fixed viewing distance of 60 cm from the eye tracker and 80 cm from the stimulus display in a dark room. The experimental setup is described in Figure 2A. The eye tracker was in front of and at the center of the LCD display. In addition, the chin rest was placed in front of the eye tracker and was set at the center viewpoint of the stimulus display. We calibrated the eye tracker using a standard five-point calibration before starting each session. Each trial began with a fixation cross presented on the monitor's center for 1 s. Afterward, the stimuli were randomly presented for 4 s in the upper, lower, left, right, or center area of the screen (Figure 2B). Participants were asked to fixate upon the central fixation cross while a stimulus was presented in the screen's periphery. Participants were instructed to refrain from blinking their eyes during the fixation and stimulus presentation periods. A blank screen with no fixation cross or stimulus (interval stage) was presented for 2 s between each trial to neutralize the participants' pupil diameter. The stimulus was repeatedly presented 15 times per condition. Thus, the experiment consisted of 150 trials: 5 VF locations (center, upper, lower, left, and right) × 2 stimulus patterns (glare and halo stimuli) × 15 trials, divided into two sessions. Participants were provided with a break of about 5 min between sessions.

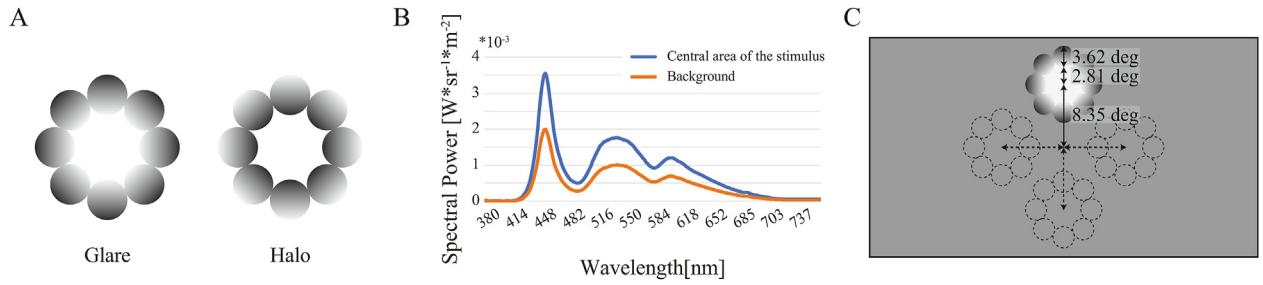

Figure 1. Experimental stimuli. (A) Glare illusion: an optical illusion using a luminance gradient that converges toward the central pattern and enhances perceptual brightness (left). Halo stimuli emit the luminance gradient toward the periphery of the stimuli and omit the glare effect (right). (B) The spectral power distribution of the central area of the stimuli and the background. (C) Stimulus size and configuration: The stimulus has eight circles with luminance gradation, which each circle located 4.62° from the display's center. The diameter of each gradation circle is at 3.62° of the visual angle. In the periphery conditions (upper, lower, left, or right visual field), the glare illusion and halo stimuli are located 8.35° from the stimulus's center to the screen's center.

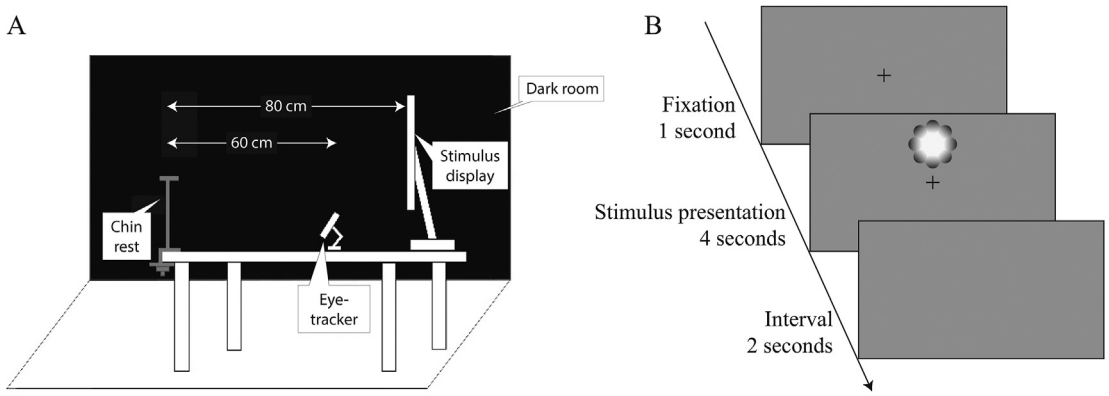

Figure 2. Experimental setup and procedure. (A) The chin rest, the fixed viewing position of participants in this study, was placed at 60 cm from the eye tracker and 80 cm from the stimulus display in a dark room. (B) The phase sequence of the experiment. Each trial started with the appearance of a fixation cross in the monitor's center for 1 s (fixation phase). Next, a stimulus (glare/halo stimuli) was presented covertly in one of four positions randomly (top, bottom, left, or right) for 4 s (stimulus presentation phase). At the end of a trial, a gray background as an interval between trials appeared for 2 s to neutralize and allow the pupillary response to return to baseline (interval phase). During the stimuli onset, observers fixated on the fixation cross and refrained from blinking their eyes.

2.4. Pupil recording and analyses

We measured pupil size and eye gaze movements using an eye-tracking system (EyeLink 1000; SR Research, Ontario, Canada) at a sampling rate of 500 Hz. The tracking was based on "pupil diameter" using the centroid mode in the device setting. The device generated pupil data in arbitrary units (pixels) and converted them to z-scores (z) during the entire experiment (two sessions) for each participant. We used cubic Hermite interpolation for the pupil data during eye blinks, which were obtained as values of zero. The analysis excluded data from trials with additional artifacts, in which the velocity change in pupil size was more than 20 z/s or the average gaze position during the presentation exceeded the radius of 2.81° (i.e., the white area of the stimulus in the center condition). Additionally, we conducted a principal component analysis at each timepoint for pupil size. We rejected trials with a Euclidian distance (calculated using the first and second principal components) exceeding ±3 σ of all trials. The average rejected trials comprised 4.6% of all trials per participant.

For the baseline correction of pupillary response, the first 0.2 s served as a baseline after the stimulus onset (the baseline period is shown as the dotted line in Figure 4), and we subtracted this baseline from any samples recorded after stimulus presentation. Then, the time course of pupillary responses for each VF location and stimulus pattern was averaged across all repeated trials. Next, we calculated early and late components [36, 37] to assess pupillary light reflex (PLR) responses and their "recovery" after the PLR. First, we averaged the pupil responses across all locations data with time series for each participant. Second, we computed the pupil slope using second-order accurate central differences to obtain the maximum pupil constriction latency (MPCL). The MPCL was defined as an initial local maximum negative value of the slope separated by ≥ 0.25 s (Figure 3). The early component was defined by the average pupil data within the window of MPCL ±0.25 (Figure 5A, red shaded area). The late component, defined as the area under the curve (AUC), was computed as follows:

$$AUC = \sum_{i=\mathrm{MPCL}}^{4} x_i - x_{\mathrm{MPCL}} \quad (1)$$

where x represents pupil size at i seconds after stimulus onset. The AUC represents a total pupil diameter increase from the PLR toward baseline pupil size (i.e., a pupil size "recovery" back to baseline).

2.5. Statistical analyses

We conducted separate statistical analyses for the center and periphery conditions. A paired-sample t-test was performed on the pupillary response in the center condition. In the periphery conditions, we conducted two-way repeated-measures analysis of variance (ANOVA) with the effect of 4 VF locations (upper, lower, left, and right) × 2 stimulus patterns (halo and glare illusion) on the pupillary response as within-subject factors. We performed Greenhouse–Geisser corrections when the results of Mauchly's sphericity test were significant. Pairwise comparisons of the main effects for multiple comparisons in the periphery conditions were tested by paired-sample t-tests. In the multiple comparisons, p-values were corrected by the Bonferroni–Holm method. The significance level (α) was set to $p < 0.05$ for all analyses. Effect sizes

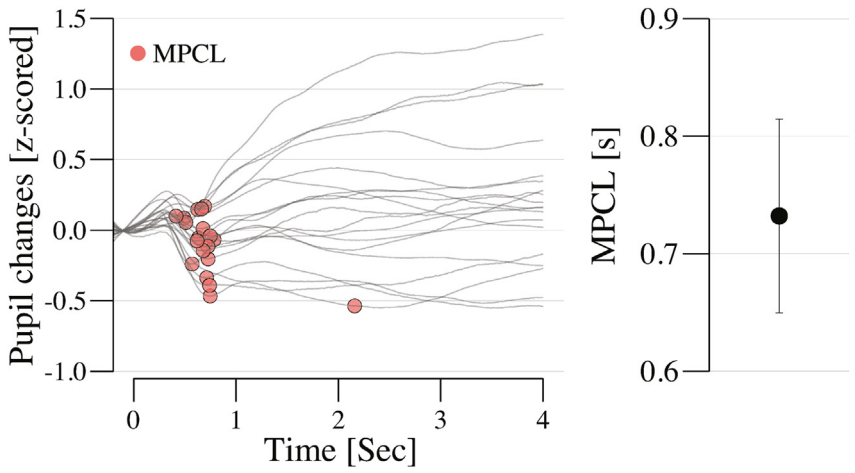

Figure 3. An initial local maximum negative value of the slope pupillary response. The maximum pupil constriction latency (MPCL) in each participant during stimulus onset for 4 s. The pupil slope was measured by second-order accurate central differences to obtain the MPCL.

were given as partial η^2 (η_p^2) for ANOVA and Cohen's d_z for the paired *t*-test analysis. We also reported the Bayes factors for estimating the relative weight of the evidence in favor of H_1 over H_0 as BF_{10} for post-hoc pairwise comparisons and *t*-tests [38]. All statistical analyses were performed using Jamovi 1.1.9.0 [39], SPSS Statistics for Windows (v26.0; IBM, Armonk, NY) [40], and the BayesFactor package (v0.9.12–4.2) [41] for R (v3.6.3; The R Foundation, Vienna, Austria) [42].

3. Results

We observed pupillary responses during the glare illusion or halo stimuli presentation at one out of five VF locations (i.e., upper, lower, left, right, and center), as shown in Figure 4. As reported previously [20, 28, 43], we confirmed that the mean pupil size from 0 s to 4 s was significantly constricted by the glare illusion in the center condition (t (18) = -3.07, p = 0.007, Cohen's d_z = 0. 704, BF_{10} = 7.36). Two-way repeated measures ANOVA on the pupillary changes in the periphery conditions revealed a significant main effect of stimulus patterns (F (1, 18) = 5.281, p = 0.034, η_p^2 = 0.227, BF_{10} = 1.658) and VF locations (F (2.37, 42.654) = 7.438, p = 0.001, η_p^2 = 0.292; BF_{10} = 49.048). However, there was no significant interaction between VF locations and stimulus patterns (F (2.597, 46.749) = 0.121, p = 0.929, η_p^2 = 0.007, BF_{10} = 0.084).

We first determined the MPCL (0.731 ± 0.361 s) to calculate the early and late components of pupillary response (see Method and Figure 3). For the center condition, there were significant differences of early (t (18) = −2.425, p = 0.026, Cohen's d_z = 0.556, BF_{10} = 2.372) and late components (t (18) = −2.344, p = 0.031, Cohen's d_z = 0.538, BF_{10} = 2.076) of pupil response between glare and halo stimuli (Figure 5A).

In the early component for the periphery conditions (Figure 5B, Table 1), two-way repeated measures ANOVA revealed a significant main effect of stimulus patterns (($1, 18$) = 8.134, p = 0.011, η_p^2 = 0.311; BF_{10} = 5.976) and VF locations (F (2.89, 52.023) = 4.356, p = 0.009, η_p^2 = 0.195, BF_{10} = 2.918). However, the post-hoc multiple comparisons for VF locations showed that no pairs of VF locations reached statistical significance ($p > 0.05$, Table 2). In addition, there was no significant interaction between VF locations and stimulus patterns (able 3; F (2.663, 47.936) = 1.066, p = 0.367, η_p^2 = 0.056, BF_{10} = 0.232).

In the late component (the AUC) for the periphery conditions, two-way repeated measures ANOVA revealed significant main effects of VF locations (F (2.128, 38.303) = 6.436, p = 0.003, η_p^2 = 0.263, BF_{10} = 70.782) and VF locations × stimulus patterns interaction (Figure 5C and Table 4) ($F(2.983, 53.691)$ = 2.883, p = 0.044, η_p^2 = 0.138, BF_{10} = 1.367). Most importantly, the post-hoc multiple comparisons for the interaction showed that the AUC for the glare illusion was significantly smaller than that

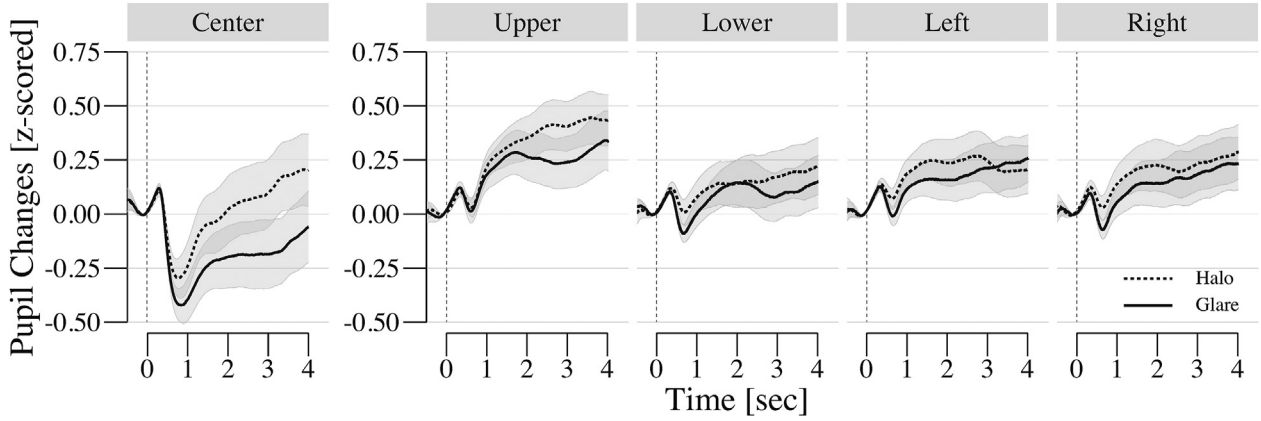

Figure 4. Pupillary changes in five locations (center, upper, lower, left, and right). The average pupil diameter change (z-score) during stimuli onset for 4 s in each position and stimuli (glare and halo stimuli). The shaded areas indicate the standard error of the mean. The dotted lines show the period for the baseline pupillary response (0.2 s).

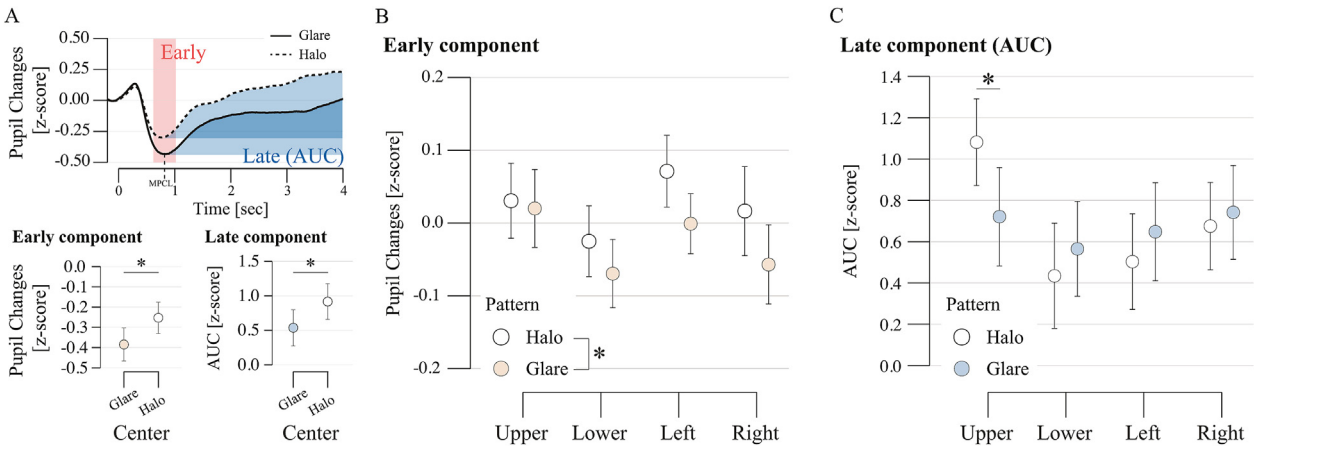

Figure 5. Early and late components of pupillary changes. (A) Computation of the early and late components of pupillary response to the glare and halo stimuli (top). The red shaded area shows the early component, which was calculated between 0 and 1 s. The late component was computed as the area under the curve (AUC) (blue shaded area). The bottom panel shows the early and late components of pupil response when the stimulus is presented at the center. **(B)** The early and **(C)** late components of pupil response in the center, upper, lower, left, and right positions. Error bars indicate standard errors of the mean.

in halo stimuli in the UVF ($t(18) = 6.847$, $p = 0.017$, $\eta_p^2 = 0.276$, $BF_{10} = 3.283$) but not in the LVF ($t(18) = 0.13$, $p = 0.723$, $\eta_p^2 = 0.007$, $BF_{10} = 0.252$), left ($t(18) = 0.466$, $p = 0.503$, $\eta_p^2 = 0.025$ $BF_{10} = 0.292$) or right VF ($t(18) = 0.798$, $p = 0.384$, $\eta_p^2 = 0.042$, $BF_{10} = 0.338$) (Table 5). Since the AUC was defined as an integral value (see Method) from the PLR to stimulus offset, a smaller AUC indicates slow recovery of pupil dilation toward the baseline pupil size. The following multiple comparisons for VF locations showed that the UVF produces a larger AUC than the LVF ($t(18) = 2.806$, $p = 0.035$, Cohen's $d_z = 0.644$), left ($t(18) = 4.091$, $p = 0.004$, Cohen's $d_z = 0.938$) and right VF ($t(18) = 2.382$, $p = 0.085$, Cohen's $d_z = 0.547$) (Table 6), in line with previous studies [12, 14, 16, 17]. We also found a significant effect of VF locations on the AUC for the halo stimulus ($F(2.533, 45.596) = 7.736$, $p = 0.001$, $\eta_p^2 = 0.301$). The post-hoc multiple comparisons for VF locations for the halo stimulus showed that the UVF produces a larger AUC than the left VF ($t(18) = 4.07$, $p = 0.004$, Cohen's $d_z = 0.934$), right ($t(18) = 3.697$, $p = 0.005$, Cohen's $d_z = 0.848$) and LVF ($t(18) = 3.388$, $p = 0.01$, Cohen's $d_z = 0.777$).

4. Discussion

This study reported pupil size during the glare illusion and halo stimuli presented in five VF locations (upper, lower, left, right, and center). We confirmed that the glare illusion induces enhanced pupillary constriction compared with halo stimuli in the center condition as reported previously [20, 28]. To assess whether there is a lower-, higher-, or combined- (lower- and higher-) level visual processing implication on pupil response to the glare illusion across VF locations, we separated the pupillary data into early and late components. The early and late components of pupillary data allowed us to assess visual processing from the temporal aspects of pupillary change. First, we found that glare-related pupil constrictions were seen in all VFs to the same degree in the center condition in the early stage. Second, VF anisotropy in the pupillary response (i.e., large pupil dilation in response to the stimuli in the UVF) was present in the late component, but not in the early component.

The early stage of the pupillary response reflects the changes in physical light intensity via lower-level visual processing [24, 44]. In addition, some studies discovered that PLR is influenced by subjective brightness perception [20, 28, 45] and visual attention on higher-level visual processing [46]. Along this line, our data seems consistent with the idea that the early component of the pupillary response involves both lower- and higher-level visual processing that creates the increased brightness perception in the glare illusion.

Previous studies have revealed that there are a smaller number of photoreceptors, acuity, and less spatial resolution with decreasing retinal eccentricity in the UVF than in the LVF [47]. Portengen et al. conducted an experiment using pupillometry and flickering stimuli in the vertical hemifield, and they found a pupillary anisotropy effect in which the UVF has greater and more sensitive pupil amplitude changes in the flickering frequency domain than the LVF [11]. In addition, paintings, images, or cartoons depicting the sun induced greater pupil constriction [20, 21, 45], most likely in response to avoid strong light from the sun. We hypothesized that the effect of pupil changes in response to the stimuli would vary across different maps due to the lower-characteristic asymmetry as well as assumptions that the light source is in the UVF [29, 31]. The current results support the idea that the interaction of lower- and higher-level visual-processing of illusory glare perception could appear as the temporal aspects of pupillary response; at the late component, glare-related pupil constrictions were larger in the UVF than in the other VFs. That is, the late component of pupillary responses might be affected by visual acuity, spatial resolution as well as brightness perception.

The visual system processes different contexts of scenes in nature to help humans understand the visual world [48]. Anatomically, sensory input from a varied VF map is processed by different areas of the primary cortex; the signal from the UVF is more dominantly processed in the ventral stream of the visual pathway [49, 50, 51]. Because of these stream differences, superior cognitive processing in the UVF and LVF depends on the type of cortical processing required for the task [49, 50]. Thus, our results imply that the cortical processing from the ventral portion may involve VF anisotropy in the pupillary response to the glare illusion. This is consistent with the increases in blood-oxygen-level-dependent (BOLD) signals in the occipitotemporal and/or collateral sulcus in response to the glare illusion [52].

The reduced pupil dilation in response to the glare illusion compared with the halo stimuli that only occurred in the UVF may be explained by the dominance of cognitive bias formed by statistical regularity in the processing of natural scenes that can represent a visual image of the UVF. The reduced pupil dilation (i.e., greater pupillary constrictions) may be observed when light sources appear in the VF other than in the UVF since these cases would be somewhat unexpected with an assumption of the light-from-above in the visual system. In the context of cognitive bias formed by statistical regularity in natural scene processing, human vision can often be exposed to light coming from the UVF [19, 29, 31, 53, 54, 55, 56]. Thus, our finding that vastly reduced pupil dilation occurs in response to the glare illusion in the UVF may be interpreted as the result of superior cognitive bias formed by statistical regularity in the processing of natural scenes in the UVF. This process may be related to the

variable response of pupil size to the probable dazzling effect geared toward preventing incapacitated vision [57].

Our study revealed that stimulus-evoked pupillary dilation and glare-related pupil constriction both point to VF anisotropy. VF anisotropy in pupil responses has been reported in the present study and elsewhere [11, 12, 14, 16, 17]. Apart from the effect of the light-from-above on the reduced pupil dilation discussed in the previous paragraph, the pupillary changes might be controlled by the nature of VF anisotropy, such as visual acuity or spatial frequency sensitivity; we cannot oppose the effect of anisotropy in VFs on pupillary response to the stimuli in each position in the present study. However, we note that our argument was under the assumption that the mechanisms that involve the brightness enhancement in the glare illusion via low- and high-order visual processing relates to the pupillary response since post-hoc multiple comparisons for the interaction exhibited a significant difference between the glare and halo stimuli only in the UVF. We have two limitations of the present study. First, we analyzed the pupillary data in the peripheral condition separately from the center condition, although our experiment designed those conditions within the same block. Thus, the higher luminance of the central white area in the center condition might affect the pupil size in the following trial. Second, another concern is that the pupillary response to the halo stimuli in the UVF might generate pupillary dilation rather than pupil constriction induced by the glare illusion. This phenomenon may be due to the better contrast sensitivity in the lower, left, and right VFs than the UVF [58]. Thus, this effect should affect the pupillary response in both the halo and glare illusion. Therefore, we believe that the differences in pupillary changes between the halo and glare illusion should still be informative. Furthermore, future studies comparing behavioral brightness data and pupillary responses could support the phenomena of higher pupillary sensitivity in UVF.

5. Conclusion

This study shows that stimulus-evoked pupillary dilation at the early component and glare-related pupil constriction in the late component occurred only in the UVF. These results indicate that the pupillary response in the glare illusion located at the UVF might relate to low- and higher-level visual processing compared with other VFs. As previously noted, the UVF's superior specific cognitive processing occurs via a different dominant visual processing stream. This may be clarified by the superior cognitive bias formed by statistical regularity in natural scene processing due to ecological factors, such as the adaptive response to the glare illusion that represents the sun as a dangerous light source. Furthermore, the present finding offers valuable insights on VF anisotropy to reduce the potential glare effect of peripheral VFs experienced in daily vision. These might be applicable in informing architectural, light, and application design of a glare source.

Declarations

Author contribution statement

Novera Istiqomah: Conceived and designed the experiments; Performed the experiments; Analyzed and interpreted the data; Contributed reagents, materials, analysis tools or data; Wrote the paper.

Yuta Suzuki, Yuya Kinzuka: Conceived and designed the experiments; Analyzed and interpreted the data; Contributed reagents, materials, analysis tools or data; Wrote the paper.

Tetsuto Minami, Shigeki Nakauch: Conceived and designed the experiments; Contributed reagents, materials, analysis tools or data; Wrote the paper.

Funding statement

This work was supported by Grants-in-Aid for Scientific Research from the Japan Society for the Promotion of Science (grant number 20H05956, 20H04273, 120219917).

Data availability statement

Data associated with this study has been deposited at Github under the url: https://github.com/suzuki970/GlarePupilAnisotropy.

Declaration of interests statement

The authors declare no conflict of interest.

Additional information

Supplementary content related to this article has been published online at https://doi.org/10.1016/j.heliyon.2022.e09772.

References

[1] K. Qian, H. Mitsudo, Spatial dynamics of the eggs illusion: visual field anisotropy and peripheral vision, Vis. Res. 177 (2020) 12–19.
[2] Y. Sakaguchi, Visual field anisotropy revealed by perceptual filling-in, Vis. Res. 43 (2003) 2029–2038.
[3] A. Bertulis, A. Bulatov, Distortions in length perception: visual field anisotropy and geometrical illusions, Neurosci. Behav. Physiol. 35 (2005) 423–434.
[4] Y. Wada, M. Saijo, T. Kato, Visual field anisotropy for perceiving shape from shading and shape from edges, Interdiscipl. Inf. Sci. 4 (1998) 157–164.
[5] J. Intriligator, P. Cavanagh, The spatial resolution of visual attention, Cognit. Psychol. 43 (2001) 171–216.
[6] F.H. Previc, The neuropsychology of 3-D space, Psychol. Bull. 124 (1998) 123–164.
[7] S. Schwartz, K. Kirsner, Laterality effects in visual information processing: hemispheric specialisation or the orienting of attention? TQ. J. Exp. Psychol. Sect. A 34 (1982) 61–77.
[8] F.H. Previc, C. Declerck, B. de Brabander, Why your "head is in the clouds" during thinking: the relationship between cognition and upper space, Acta Psychol. 118 (2005) 7–24.
[9] R. Arnheim, J.J. Gibson, The perception of the visual world, J. Aesthet. Art Critic. 11 (1952) 172.
[10] F.H. Previc, Functional specialization in the lower and upper visual fields in humans: its ecological origins and neurophysiological implications, Behav. Brain Sci. 13 (1990) 519–542.
[11] B.L. Portengen, et al., Blind spot and visual field anisotropy detection with flicker pupil perimetry across brightness and task variations, Vis. Res. 178 (2021) 79–85.
[12] S. Hong, J. Narkiewicz, R.H. Kardon, Comparison of pupil perimetry and visual perimetry in normal eyes: decibel sensitivity and variability, Invest. Ophthalmol. Visual Sci. 42 (2001) 957–965.
[13] M. Naber, et al., Gaze-contingent flicker pupil perimetry detects scotomas in patients with cerebral visual impairments or glaucoma, Front. Neurol. 9 (2018) 558.
[14] F. Sabeti, A.C. James, T. Maddess, Spatial and temporal stimulus variants for multifocal pupillography of the central visual field, Vis. Res. 51 (2011) 303–310.
[15] K. Skorkovská, H. Wilhelm, H. Lüdtke, B. Wilhelm, A. Kurtenbach, Investigation of summation mechanisms in the pupillomotor system, Graefe's Arch. Clin. Exp. Ophthalmol. 252 (2014) 1155–1160.
[16] L. Tan, M. Kondo, M. Sato, N. Kondo, Y. Miyake, Multifocal pupillary light response fields in normal subjects and patients with visual field defects, Vis. Res. 41 (2001) 1073–1084.
[17] H. Wilhelm, et al., Pupil perimetry using M-sequence stimulation technique, Invest. Ophthalmol. Visual Sci. 41 (2000) 1229–1238.
[18] J. Zihl, P. Lissy, E. Pöppel, Brightness perception in the visual field - effects of retinal position and adaptation level, Psychol. Res. 41 (1980) 297–304.
[19] M.E. McCourt, B. Blakeslee, G. Padmanabhan, Lighting direction and visual field modulate perceived intensity of illumination, Front. Psychol. 4 (2013) 1–6.
[20] B. Laeng, T. Endestad, Bright illusions reduce the eye's pupil, Proc. Natl. Acad. Sci. U. S. A. 109 (2012) 2162–2167.
[21] P. Binda, M. Pereverzeva, S.O. Murray, Pupil constrictions to photographs of the sun, J. Vis. 13 (2013) 1–9.
[22] E. Irene, O.L. Loewenfeld, The pupil: anatomy, physiology, and clinical applications, Br. J. Ophtalmol. 85 (2001) 121.
[23] J. Rajkowski, P. Kubiak, G. Aston-Jones, Correlations between locus coeruleus (LC) neural activity, pupil diameter and behavior in monkey support a role of LC in attention, Soc. Neurosci. Abstr. 19 (1993) 974.
[24] S. Mathôt, Pupillometry: psychology, physiology, and function, J. Cognit. 1 (2018) 1–23.
[25] M. Jepma, S. Nieuwenhuis, Pupil diameter predicts changes in the exploration-exploitation trade-off: evidence for the adaptive gain theory, J. Cognit. Neurosci. 23 (2011) 1587–1596.
[26] M.S. Gilzenrat, S. Nieuwenhuis, M. Jepma, J.D. Cohen, Pupil diameter tracks changes in control state predicted by the adaptive gain theory of locus coeruleus function, Cognit. Affect Behav. Neurosci. 10 (2010) 252–269.
[27] G. Aston-Jones, J.D. Cohen, An integrative theory of locus coeruleus-norepinephrine function: adaptive gain and optimal performance, Annu. Rev. Neurosci. 28 (2005) 403–450.

[28] Y. Suzuki, T. Minami, B. Laeng, S. Nakauchi, Colorful glares: effects of colors on brightness illusions measured with pupillometry, Acta Psychol. 198 (2019), 102882.
[29] M. de Montalembert, L. Auclair, P. Mamassian, Where is the sun" for hemi-neglect patients? Brain Cognit. 72 (2010) 264–270.
[30] D. Zavagno, O. Daneyko, When figure-ground segmentation modulates brightness: the case of phantom illumination, Acta Psychol. 129 (2008) 166–174.
[31] J. Sun, P. Perona, Where is the sun? Nat. Neurosci. 1 (1998) 183–184.
[32] S. He, P. Cavanagh, J. Intriligator, Attentional resolution and the locus of visual awareness, Nature 6598 (1996) 334–337.
[33] D. Zavagno, The phantom illumination illusion, Percept. Psychophys. 67 (2005) 209–218.
[34] Y. Kinzuka, F. Sato, T. Minami, S. Nakauchi, Effect of glare illusion-induced perceptual brightness on temporal perception, Psychophysiology 58 (2021).
[35] D.H. Brainard, The psychophysics toolbox, Spatial Vis. 10 (1997) 433–436.
[36] V.L. Kinner, et al., What our eyes tell us about feelings: tracking pupillary responses during emotion regulation processes, Psychophysiology 54 (2017) 508–518.
[37] M.M. Bradley, L. Miccoli, M.A. Escrig, P.J. Lang, The pupil as a measure of emotional arousal and autonomic activation, Psychophysiology 45 (2008) 602–607.
[38] S. Andraszewicz, et al., An introduction to bayesian hypothesis testing for management research, J. Manag. 41 (2015) 521–543.
[39] J. Love, D. Dropmann, R. Selker, The Jamovi Project (2021), 2021.
[40] SPSS Inc., SPSS Statistics for Windows, 2008.
[41] R.D. Morey, Computation of Bayes Factors for Common Designs [R Package BayesFactor version 0.9.12-4.2]. CRAN Repository, 2019.
[42] R Core Team. *R*, A Language and Environment for Statistical Computing, 2020 (URL: https://www.r-project.org/.
[43] D. Zavagno, L. Tommasi, B. Laeng, The eye pupil's response to static and dynamic illusions of luminosity and darkness, Iperception 8 (2017).
[44] P. Mamassian, M. de Montalembert, A simple model of the vertical-horizontal illusion, Vis. Res. 50 (2010) 956–962.
[45] M. Naber, K. Nakayama, Pupil responses to high-level image content, J. Vis. 13 (2013) 1–8.
[46] J.S. Pointer, R.F. Hess, The contrast sensitivity gradient across the human visual field: with emphasis on the low spatial frequency range, Vis. Res. 29 (1989) 1133–1151.
[47] A. Goldstein, H. Babkoff, A comparison of upper vs. lower and right vs. left visual fields using lexical decision, Q. J. Exp.Psychol. Sect. A: Hum. Exp. Psychol. 54 (2001) 1239–1259.
[48] N. Rubin, K. Nakayama, R. Shapley, Enhanced perception of illusory contours in the lower versus upper visual hemifields, Science (1979) 271 (1996) 651–653.
[49] D.J. Felleman, D.C. Van Essen, Distributed hierarchical processing in the primate cerebral cortex, Cerebr. Cortex 1 (1991) 1–47.
[50] M.I. Sereno, et al., Borders of multiple visual areas in humans revealed by functional magnetic resonance imaging, Science (1979) 268 (1995) 889–893.
[51] Caitlin O'Connell, Leon C. Ho, Matthew C. Murphya, Ian P. Conner, Gadi Wollstein, Rakie Chamb, K.C. Chan, Structural and functional correlates of visual field asymmetry in the human brain by diffusion kurtosis MRI and functional MRI, Physiol. Behav. 176 (2016) 100–106.
[52] U. Leonards, T. Troscianko, F. Lazeyras, V. Ibanez, Cortical distinction between the neural encoding of objects that appear to glow and those that do not, Br. J. Brain Res. Cognit. Brain Res 24 (2005) 173–176.
[53] V.S. Ramachandran, Perception of shape from shading, Nature 331 (1988) 163–166.
[54] P. Mamassian, R. Goutcher, Prior knowledge on the illumination position, Cognition 1 (2001) 1–9.
[55] A.J. Schofield, P.B. Rock, M.A. Georgeson, Sun and sky: does human vision assume a mixture of point and diffuse illumination when interpreting shape-from-shading? Vis. Res. 51 (2011) 2317–2330.
[56] J.V. Stone, I.S. Kerrigan, J. Porrill, Where is the light? Bayesian perceptual priors for lighting direction, Proc. Biol. Sci. 276 (2009) 1797–1804.
[57] Y. Lin, et al., Eye movement and pupil size constriction under discomfort glare, Invest. Ophthalmol. Vis. Sci. 56 (2015) 1649–1656.
[58] M.M. Himmelberg, J. Winawer, M. Carrasco, Stimulus-dependent contrast sensitivity asymmetries around the visual field, J. Vis. 20 (2020) 1–19.